Modified Discrete Wavelet Transformation to Compress DICOM Medical Images with Run-Length Encoding

T.M. Embuldeniya, R. G. N. Meegama
Department of Computer Science, Faculty of Applied Sciences,
University of Sri Jayewardenepura, Sri Lanka.

***Abstract*—With rapid advancements in medical imaging technology, a substantial amount of image data has been produced to assist clinical diagnostics. Nevertheless, storing and transmitting medical images with high-resolution content presents a formidable challenge that needs to be addressed. This study proposes a technique to compress DICOM images using a Modified variant of Discrete Wavelet Transform (MDWT) including Run-Length Encoding and DEFLATE algorithm. The proposed mechanism decomposes a DICOM image into its frequency sub-bands, namely, approximation (LL), horizontal detail (LH), vertical detail (HL), and diagonal detail (HH) coefficients which are then thresholded and quantized in an adaptive manner using uniform scalar quantization. The quantized coefficients are run-length encoded with a modified scheme to traverse the data including linear, diagonal, and spiral approaches. Subsequently, DEFLATE algorithm-based compression is performed for further reduction in data volume. Results indicate a noteworthy improvement in compression ratio with the modifications while preserving a high level of detail.**

***Index Terms*—Discrete Wavelet Transform (DWT), Run-length Encoding (RLE), Huffman Encoding, Uniform Scalar Quantization**

I. Introduction

Images play a pivotal role in medical data representation and diagnostics. The number of bits required to represent an image varies based on the amount of contained information, resolution, and the bit depth. To be efficient while working with complex types of data, compression is extremely beneficial in storage aspects and transmission. This is particularly important when dealing with DICOM (Digital Imaging and Communications in Medicine) images as they tend to have pixels with high bit depth, often 16-bit from MRI (Magnetic Resonance Imaging), CT (Computerized Tomography), and other scanning devices. Moreover, the volume of medical imaging data generated daily is significantly increasing [1]. Although the cost of storage and computing resources has decreased with technological development, managing extensive records, communication, and other medical analytics related to DICOM images can still present challenges.

Maintaining large records of medical images can pave the path to diagnostics and research on the evolution of diseases over time [2]. Also, fast communication is quintessential in telemedicine solutions, especially for an underprivileged community with little or no access to expert medical practitioners.

Representing images with the fewest possible bits while maintaining the essential details and visual fidelity can be considered as image compression. It is achieved by exploiting redundancies that naturally occur in image data and eliminating them to form a compact representation. Three types of redundancies are commonly exploited in digital images. Mainly, **coding redundancy** occurs when some symbols or values in an image are more likely to occur than others. Coding methods that assign shorter codes to symbols which are more probable to occur can take advantage of this phenomenon and lower the average number of bits required to represent a pixel. This process is reversible thus no information loss can occur. Run length encoding (RLE), Arithmetic encoding, Lempel-Ziv-Welch (LZW) and Huffman encoding are some techniques that leverage such properties. Secondly, **Inter pixel Redundancy** refers to the correlation between pixels exists and is not statistically independent. This interconnectedness allows the value of a given pixel to be determined from its neighbors. Finally, **Psycho-Visual Redundancy**; results from the way of human visual system interprets optic data along with the limited capability of the human brain to comprehend fine details, colors, and spatial frequencies. Effectively harnessing these constraints can reduce the data required to represent the image [3]. Transform coding techniques such as the discrete cosine transform (DCT) used in JPEG and the wavelet transform used in JPEG 2000 [4], convert the image from the spatial domain to the frequency domain allowing efficient exploitation of such redundancies, that otherwise might be hard to perceive.

Image compression techniques can be broadly categorized as either **lossless** or **lossy**. Lossless methods minimize the data volume of the image without sacrificing quality. Encoding techniques are generally lossless. In contrast, lossy compression omits certain information that is less significant

Correspondence: Thisura Embuldeniya (E-mail: tisura.e@gmail.com)
Received: 16-06-2024 **Revised:** 12-08-2024 **Accepted:** 09-09-2024
Thisura Embuldeniya and R. G. N. Meegama are from University of Sri Jayewardenepura (tisura.e@gmail.com, rgn@sjp.ac.lk)
DOI: https://doi.org/10.4038/icter.v18i2.7287
The 2025 Special Issue contains the full papers of the abstracts published at the 24th ICTer International Conference.

causing a quality degradation in the reconstructed when compared with the original image [3]. Transform coding methods like the discrete cosine transform (DCT) and wavelet transform can produce lossy results by discarding some information after the transformation.

Achieving high-fidelity compression is paramount in medical imaging, necessitating algorithms to prioritize image quality while reducing the data volume. This study evaluates the effectiveness of the various modifications to Discrete Wavelet Transform-based compression for medical DICOM images.

II. Related work

In the field of image compression, the discrete wavelet transform (DWT) has gained momentous attention due to its ability to provide better compression with superior quality. M. Mozammel et al., [5] have proposed an image compression method based on wavelet transformation and thresholding. In the proposed method, firstly the image was decomposed into wavelet coefficients, and hard thresholding was applied. The thresholded coefficients were then encoded in a lossless manner. Based on the results, a threshold value of 30 is suggested for their proposed method, which can compress a set of raw test images in BMP (bitmap) format with a size of 47KB to 1.94KB with a compression ratio (CR) of 24.22:1 and a Peak Signal to Noise Ratio (PSNR) of 19.86dB. Also, a comparison with the JPEG standard compression signifies that the same image yields a 3.38KB compressed size, 13.90:1 compression ratio, and a PSNR of 24.42 dB.
JPEG standard which is one of the most widely used image compression utilizes the transformation technique known as Discrete cosine transform (DCT). Anilkumar Katharotiya et al., [6] Kiran Bindu et al., [7] performed comparative studies between DCT and DWT to experimentally observe their advantages and drawbacks. Anilkumar Katharotiya et al., proposed mechanisms to simulate and observe the differences between DCT and DWT, where the overall process was segregated into encoding and decoding systems. One notable element in implementing DCT was breaking the image into blocks which helps the algorithm to exploit local spatial redundancies. The proposed method breaks the image into NxN blocks where N can be 4, 8, 16, etc. Due to this, blocking artifacts were visible in the results of DCT degrading the overall quality. According to their conclusions, DWT had performed better in quality, but in performance time, DCT was better. Kiran Bindu et al., also conducted experiments to compare DCT and DWT, along with a hybrid DCT-DWT compression technique. Their conclusions also indicated similar outcomes for comparing DWT with DCT.

In the medical imaging field, researchers have conducted numerous studies to investigate the effectiveness of DWT in compressing DICOM images specifically, employing different approaches. Ruchika et al., [8] proposed a DICOM image compression method based on DWT and Huffman encoding. The compression process determines the decomposition level based on the entropy of the image. Once decomposed, hard thresholding was applied and Huffman encoded to reduce the data redundancy. Experiments had been conducted using 3 wavelets; Haar, Bior 4.4, and Sym8, and had received mixed results with slight variations between the wavelets and the type of the image. Overall, it was concluded that the algorithm performed well for all images. Paul Ammah et al., [9] had implemented a compression algorithm using DWT and vector quantization (VQ). Vector quantization is a lossy compression technique and in their proposed mechanism they aimed to balance the quality with high compression ratios. Another noteworthy fact is that they have performed pre-processing to remove noise, specifically salt and pepper noises that were present in the images. According to their observations, these noises were primarily found in ultrasound images but negligible in other types. Once the images were pre-processed, decomposition using DWT and thresholding was applied. The resultant coefficients were vector quantized and Huffman encoded. Their experiments produced favorable outcomes for the efficacy of the hybrid DWT-VQ approach.

III. Methodology

The proposed method with modifications can be divided into 6 subprocesses as depicted in Figure 1. Under compression, first, the images were prepared by separating pixel (spatial) data and metadata. Next, Discrete wavelet transform was applied, and the resulting coefficients were thresholded with hard thresholding. Following this, quantization was done using Uniform Scalar Quantization with an adaptively chosen quantization step size for each image. As the Final step in compression, the quantized coefficients were entropy encoded with Run-Length Encoding (RLE) and DEFLATE based gzip algorithm which then can be either stored or transmitted.

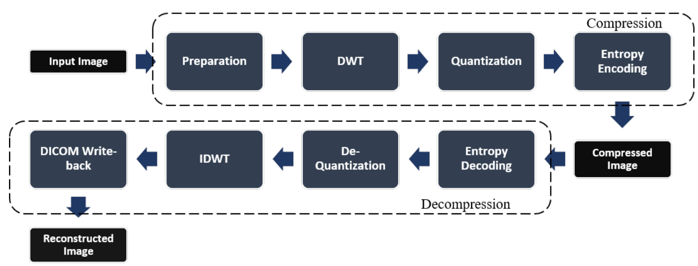

Fig. 1: Workflow of the proposed algorithm

The inverse of the compression process can be applied to obtain the reconstructed image. Under decompression, the data is initially entropy decoded using the INFLATE functionality in DEFLATE algorithm following the reverse process of RLE. Then the proceedings are de-quantized. Since Uniform Scalar Quantization was used, de-quantization can be done by performing element-wise multiplication of the decoded data matrix with the quantization step size. It converts the coefficients to their original form enabling inverse discrete wavelet transformation (IDWT) to be applied. After applying IDWT, a DICOM write-back is performed by combining reconstructed image data with the separately stored metadata.

A. *Discrete Wavelet Transformation (DWT) and Thresholding*

In practical applications, DWT is computed through multi-level decomposition, which involves applying low-pass and high-pass filters within filter banks to a signal that extracts the approximation and detail coefficients. Filter banks are an array of pass filters that allow signals with a certain frequency range and reject other frequencies outside that range. There are notably two types of filter banks: analysis filter banks, which separate the input signal into multiple subbands of the original signal, and synthesis filter banks, which merge subbands into a single wideband reconstructing the input signal [10].

The filtered component from a filter undergoes a down-sampling by a factor of 2 to eliminate redundant information, particularly when a 2-channel filter bank is used. In DWT this process is iterated to remove high frequency components at each decomposition level. DWT-based image compression algorithms decompose an image into four frequency bands by analyzing the image as a 2D signal that changes vertically and horizontally. This decomposition yields a set of wavelet coefficients representing specific details of the image; the approximation for the original image (LL), vertical details (HL), horizontal details (LH), and diagonal details (HH). Mathematically, in a 2-D wavelet transform, these 4 components can be defined using the product of a one-dimensional scaling function φ and the orresponding wavelet ψ [10].

- Approximation Details (LL) - $\varphi(x, y) = \varphi(x)\varphi(y)$
- Horizontal Details (HL) - $\psi^H(x, y) = \psi(x)\varphi(y)$
- Vertical Details (LH) - $\psi^V(x, y) = \varphi(y)\psi(x)$
- Diagonal Details (HH) - $\psi^D(x, y) = \psi(x)\psi(y)$

In the proposed method, coefficients were generated using MATLAB's built-in functions [11] followed by the thresholding process.

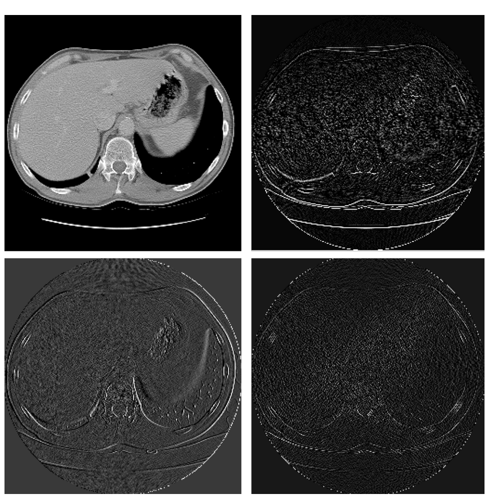

Fig. 2: Decomposition of a CT image

Here hard thresholding was applied as defined in Equation 1, [12] and the threshold level (λ) was chosen based on the required amount (fraction) of the coefficients to retain. It was obtained under two different criteria; either from user input or determined by the algorithm based on the mean square error.

$$\hat{w}_{j,k} = \begin{cases} w_{j,k} & \text{if } |w_{j,k}| \geq \lambda \\ 0 & \text{if } |w_{j,k}| < \lambda \end{cases} \tag{1}$$

The threshold level was determined in a way where the coefficients closer to 0 were prominently affected by sorting in ascending order. This approach resulted in better information retention.

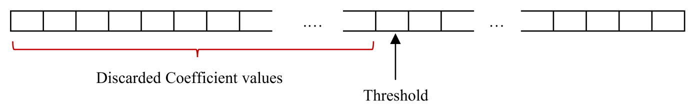

Fig. 3: Abstract Depiction of Discarded Coefficients

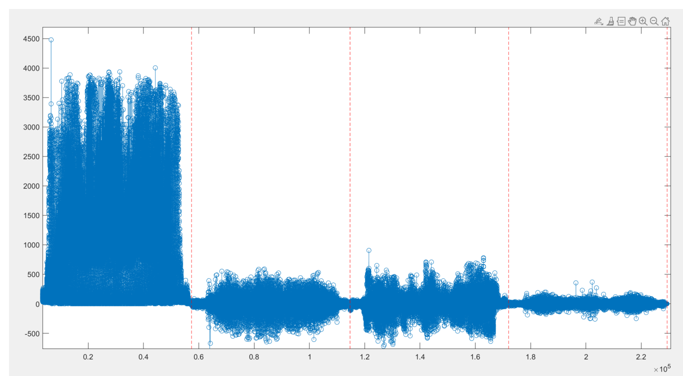

Fig. 4: Distribution of Level 1 Wavelet Coefficients of an MRI image (All 4 sub bands – LL, HL, LH, HH)

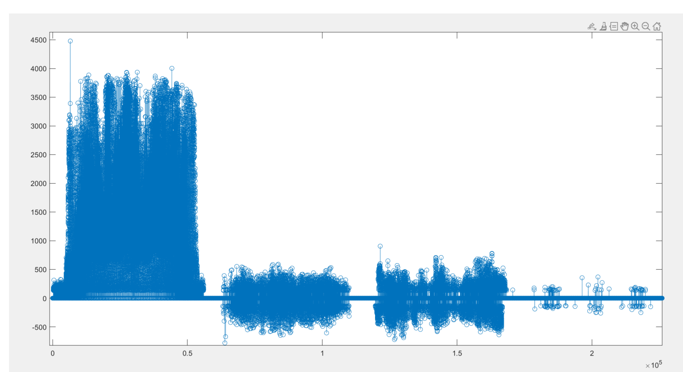

Fig. 5: Wavelet Coefficients after thresholding of the same MRI image (retention – 0.2)

B. *Quantization*

Quantization allows the DWT coefficients to be presented in a compact form. It reduces the precision of the coefficients and the number of bits required to represent them. This enhances efficiency in entropy encoding due to reduced precision resulting a lower entropy. But it is a lossy process, which introduces errors by discarding fine details. The level of quantization applied has a trade-off between image quality and compression ratio. Higher levels of quantization result in higher compression ratios with lower image quality.

Various quantization techniques are available that can be employed, including uniform scalar quantization, Lloyd-Max quantization, and vector quantization. In uniform scalar quantization, the given range of values is equally divided into a set of discrete levels, while keeping a uniform interval between each level denoted as the quantization step size [13]. In Lloyd-Max Quantization, the step size is altered based on the probability density of the input values and iteratively adjusted to minimize the Mean Squared Error (MSE) between the original and quantized values. The process begins by determining a predefined number of quantization levels required and allocates the levels depending on the distribution of the values. For a given subrange if there are a higher number of data points then more quantization levels would be imposed, in the attempt to minimize the MSE. In vector quantization, the values are divided into clusters, where each cluster is represented by a centroid or a codeword. Here the codewords are selected minimizing the error between the original vectors and their quantized values. The k-means algorithm is commonly used in implementing vector quantization.

In the proposed approach uniform scalar quantization is applied where the quantization step size is determined adaptively for a given image. To minimize the computational overhead when iteratively searching for an optimal step value, pre-defined ranges and a technique similar to binary search are utilized.

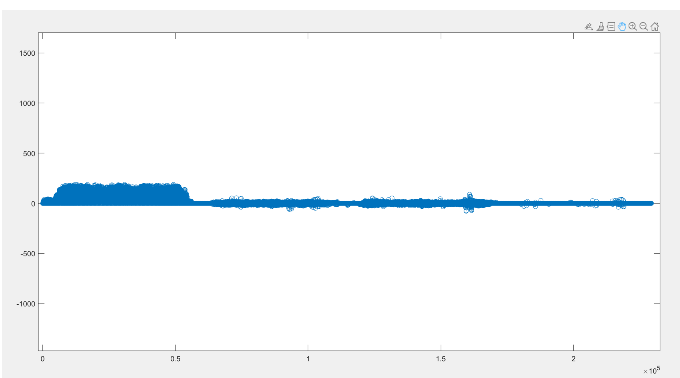

Fig. 6: Wavelet Coefficients after quantizing (q = 20) compact form of the same MRI image

C. Entropy Encoding

Once the DWT coefficients are quantized, they need to be entropy encoded to archive the best-compressed form suitable for storage or transmission. Out of the available entropy encoding mechanisms, run-length encoding is first applied to the coefficient matrices and further compressed by using the DEFLATE algorithm-based gzip compression technique. Run-length encoding (RLE) reduces the size of a file or data stream by storing a sequence of identical values as a single element followed by the number of repetitions that occur in sequence. This method is particularly effective for compressing data that contains long runs of repeated values. For example, the string "AAABBBCCCCD" could be compressed to "A3B3C4D1". For real-valued matrices, this method can be applied by traversing the matrix [14] with a defined manner and recording each element along with its recurrences. This can be useful if the matrix has a lot of repeating elements, but its effectiveness wanes when confronted with values exhibiting high entropy leading to an increase in size and negatively impacting the compression.

In the proposed approach RLE was applied for the coefficient matrices under three different methods and their effectiveness was experimented with. It was identified that the approximation coefficient matrix (LL) has exhibited a high entropy as it contains most of the image information and yielded undesirable results when applying RLE, prompting its exclusion from the process. Other matrices were concatenated horizontally and traversed as illustrated below. The following Figure 7 depicts three example matrices utilized in demonstrating the traversal mechanisms.

$$\begin{bmatrix} 1 & -5 & -6 & -3 \\ 2 & 2 & 3 & 44 \\ 3 & 5 & 40 & 0 \\ 0 & 0 & 0 & 0 \end{bmatrix} \quad \begin{bmatrix} 1 & -1 & -6 & -3 \\ 1 & 1 & 0 & 41 \\ 2 & 0 & 0 & 0 \\ 0 & 0 & 0 & 0 \end{bmatrix} \quad \begin{bmatrix} 7 & -7 & -5 & -3 \\ 1 & 0 & 0 & 10 \\ 0 & 0 & 0 & 0 \\ 0 & 0 & 0 & 0 \end{bmatrix}$$

A B C

Fig. 7: Example Matrices

a) Linear traversal (Figure 8)

$$\begin{bmatrix} 1 & -5 & -6 & -3 & 1 & -1 & -6 & -3 & 7 & -7 & -5 & -3 \\ 2 & 2 & 3 & 44 & 1 & 1 & 0 & 41 & 1 & 0 & 0 & 10 \\ 3 & 5 & 40 & 0 & 2 & 0 & 0 & 0 & 0 & 0 & 0 & 0 \\ 0 & 0 & 0 & 0 & 0 & 0 & 0 & 0 & 0 & 0 & 0 & 0 \end{bmatrix}$$

Fig. 8: Linear Traversal of Concatenated Matrix ABC

b) Diagonal traversal (Figure 9)

$$\begin{bmatrix} 1 & -5 & -6 & -3 & 1 & -1 & -6 & -3 & 7 & -7 & -5 & -3 \\ 2 & 2 & 3 & 44 & 1 & 1 & 0 & 41 & 1 & 0 & 0 & 10 \\ 3 & 5 & 40 & 0 & 2 & 0 & 0 & 0 & 0 & 0 & 0 & 0 \\ 0 & 0 & 0 & 0 & 0 & 0 & 0 & 0 & 0 & 0 & 0 & 0 \end{bmatrix}$$

Fig. 9: Diagonal Traversal of Concatenated Matrix ABC

c) Spiral traversal (Figure 10)

$$\begin{bmatrix} 1 & -5 & -6 & -3 & 1 & -1 & -6 & -3 & 7 & -7 & -5 & -3 \\ 2 & 2 & 3 & 44 & 1 & 1 & 0 & 41 & 1 & 0 & 0 & 10 \\ 3 & 5 & 4 & 0 & 2 & 0 & 0 & 0 & 0 & 0 & 0 & 0 \\ 0 & 0 & 0 & 0 & 0 & 0 & 0 & 0 & 0 & 0 & 0 & 0 \end{bmatrix}$$

Fig. 10: Spiral Traversal of Concatenated Matrix ABC

Once RLE was performed, the results were further encoded employing the DEFLATE algorithm using MATLAB's built-in gzip function. DEFLATE algorithm combines LZ77 (Lempel-Ziv 77) and Huffman encoding techniques to deliver high data compression [15].

D. Performance evaluation metrics

Several evaluation metrics were used to evaluate the effectiveness of the modifications. Mean Square Error (MSE) and Root Mean Square Error (RMSE) are two common metrics used in image comparison. MSE measures the average squared variation in pixel values between two images. To calculate it, both should ideally be in the same resolution or a sampling technique is necessary to match one with the other.

A lower MSE value indicates a smaller difference between the two images. However, the squared variation may not directly reflect the difference. RMSE is a more directly interpretable measure, derived by obtaining the square root of the MSE value and is scaled to the dynamic range of the image, making it more meaningful for assessing pixel differences.

$$MSE = \frac{1}{M \times N} \sum_{x=1}^{M} \sum_{y=1}^{N} (I_1(x,y) - I_2(x,y))^2 \tag{2}$$

$$RMSE = \sqrt{MSE} \tag{3}$$

Where:
$I_1(x,y)$ represents the pixel value at location (x,y) in the first image.
$I_2(x,y)$ represents the pixel value at location (x,y) in the second image.
$M \times N$ is the total number of pixels in the image.

The Peak Signal-to-Noise Ratio (PSNR) is another metric widely used for image comparison. It signifies the ratio of a signal's maximal power to the power of distorted noise that impairs the accuracy of its representation and can be computed as depicted in Equation 4.

$$PSNR = 10 \log_{10} \left(\frac{{MAX_f}^2}{MSE} \right) \tag{4}$$

Where:
MAX_f is the maximum possible value of the image pixel;
For a 16-bit image, $MAX_f = (2^{16} - 1)$.

Higher PSNR values indicate better image quality, while lower values suggest substantial distortions or compression artifacts.

Mean Absolute difference (Mean AD) also assesses the averaged pixel variance by measuring the absolute difference between the pixel values and averaging them (Equation 5). Mean AD is less sensitive to large variations compared to RMSE as it gives higher weight for extensive errors through squaring. Both are used to evaluate the difference between images, where Mean AD provides a straightforward measure of the average difference between the pixels while RMSE takes into consideration the magnitude of the error distribution.

$$MeanAD = \frac{1}{M \times N} \sum_{x=1}^{M} \sum_{y=1}^{N} |(I_1(x,y) - I_2(x,y))| \tag{5}$$

Although the above metrics are popular in assessing quality, they do not always correlate well with human perception. For that, the Structural Similarity Index (SSIM) can be used to assess two images by considering perceived changes in luminance, contrast, and structural information computed on various windows of an image. It can be defined as in Equation 6 for two windows x and y [9].

$$SSIM_{(x,y)} = \left[\frac{2\mu_x \mu_y}{{\mu_x}^2 + {\mu_y}^2} \right] \times \left[\frac{2\sigma_{xy}}{{\sigma_x}^2 + {\sigma_y}^2} \right] \tag{6}$$

Where:
μ_x, μ_y represent the means of x and y.
${\sigma_x}^2, {\sigma_y}^2$ represent the standard deviations of x and y.
σ_{xy} represents the covariance between x and y.

Mean and standard deviation can be computed as follows for windows x and y.

$$\mu_x = \frac{1}{K} \sum_{i=1}^{K} x_i \quad \text{and} \quad \sigma_x = \left[\frac{1}{K-1} \sum_{i=1}^{K} (x_i - \mu_x)^2 \right]^{1/2} \tag{7}$$

$$\mu_y = \frac{1}{K} \sum_{i=1}^{K} y_i \quad \text{and} \quad \sigma_y = \left[\frac{1}{K-1} \sum_{i=1}^{K} (y_i - \mu_y)^2 \right]^{1/2} \tag{8}$$

Where:
x_i and y_i represent the i^{th} pixel intensity in image windows x and y, respectively.

A SSIM index of 1 represents a perfect match, where values closer to 1 indicate greater similarity between the images.

Finally, effectiveness of the algorithm was evaluated using Compression Ratio (CR) and defined as follows.

$$\text{Compression Ratio} = \frac{\text{Original Size}}{\text{Compressed Size}} \tag{9}$$

IV. RESULTS AND DISCUSSION

For Experiments, 16 DICOM images were obtained from a free online DICOM repository; cancerimagingarchive.net [16] in 16-bit uncompressed format taken from CT and MRI scanning devices. These images were compressed using the implemented general version of the DWT compression algorithm along with its proposed modifications. The results were obtained under two criteria: by variating the threshold rate and assigning a target MSE value.

A. *Varying Threshold Rate*

As mentioned in the methodology, the algorithm requires the degree of thresholding desired by the user. In this implementation, it is identified as the threshold rate, which determines the required amount (fraction) of the coefficients to retain. The images were compressed by varying the threshold rate from 0.2 to 0.99 with a step size of 0.03. Subsequently, for a given threshold rate, all readouts from the image set regarding a certain metric (such as RMSE) were averaged and compared. (Figure 11)

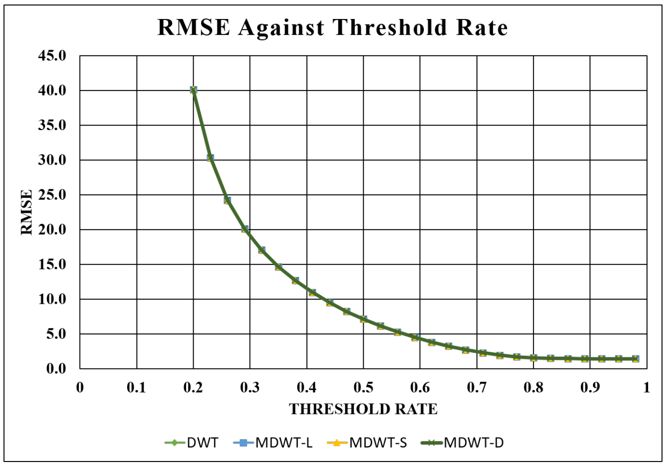

Fig. 11: RMSE against Threshold rate

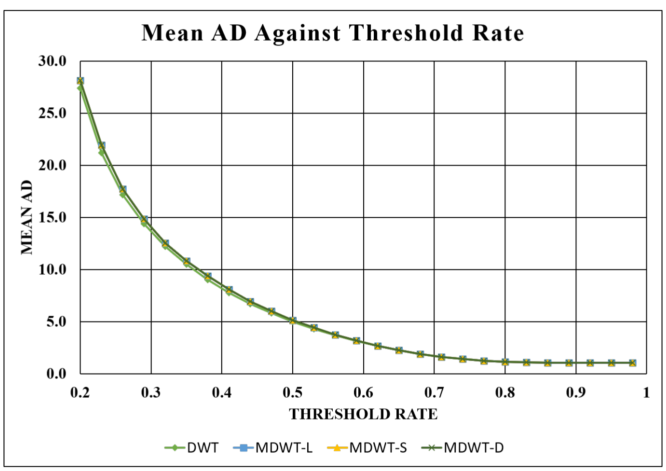

Fig. 12: Mean AD against Threshold rate

B. *Performance against a given Target MSE*

By the second evaluation criterion, the algorithm will seek for the near-best compression ratio to a given MSE. Once set for a target value, the image reconstruction quality will be nearly identical among all the implemented variations. Thus, the compression ratio achieved by each can be compared.

Here the general DWT algorithm is denoted as DWT and the modified version is denoted as MDWT along with its variation. MDWT with linear traversal (MDWT-L), MDWT with Diagonal traversal (MDWT-D), MDWT with Spiral

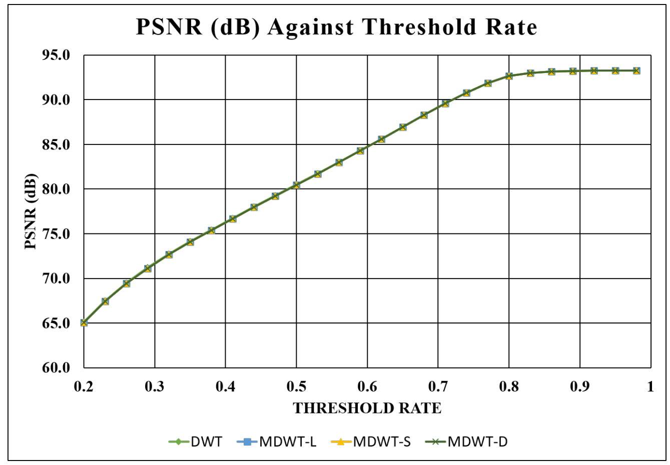

Fig. 13: PSNR against Threshold rate

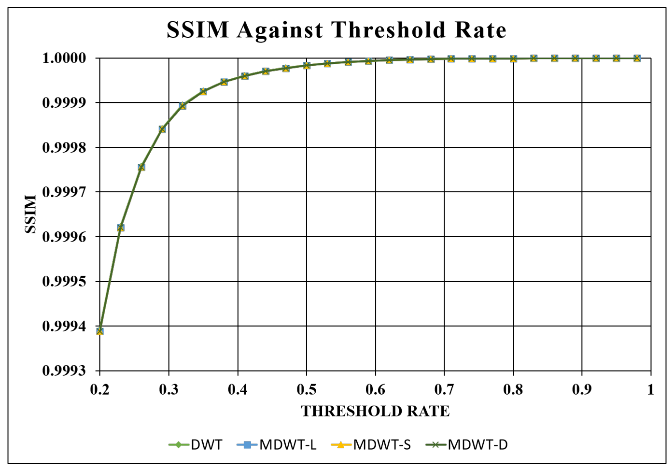

Fig. 14: SSIM against Threshold rate

traversal (MDWT-S).

In the experimental observations, all variants have maintained comparable image quality according to the first criterion. However, noticeable improvements were observed in compression ratio of the modified versions for a considerable range of thresholding. Since there is no perceptible discrepancy in quality metrics (RMSE, PSNR, SSIM, Mean AD), it can be concluded that no degradation of quality has occurred when aiming for higher compression ratios. The second criterion further validates the previous results with added accuracy as using a set target for MSE, all the versions were compelled to produce almost identical reconstruction while striving to achieve a near-best compression ratio. Experiments substantiate that the compression ratios are superior to the general DWT algorithm for both MSE $\approx$ 100 and MSE $\approx$ 225.(Figure 17, 18) The wavelet 'db1' was used in all implementations.

To evaluate the overall complexity including time and other computational resources for the proposed modifications, the complexity of the implemented custom code and the utilized MATLAB built-in functions need to be examined.

The algorithm includes components for run-length encoding

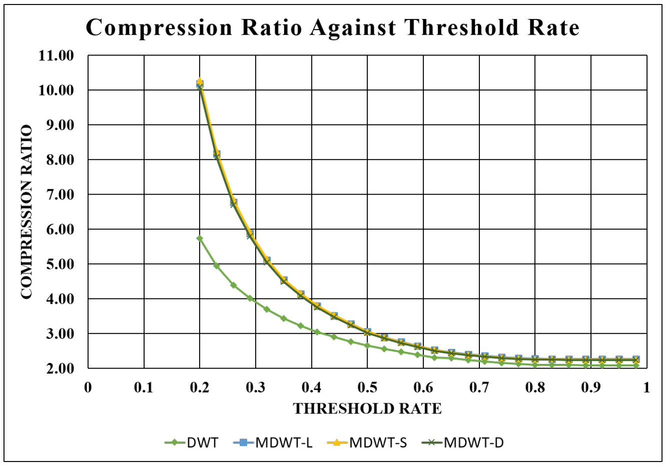

Fig. 15: Compression Ratio against Threshold rate

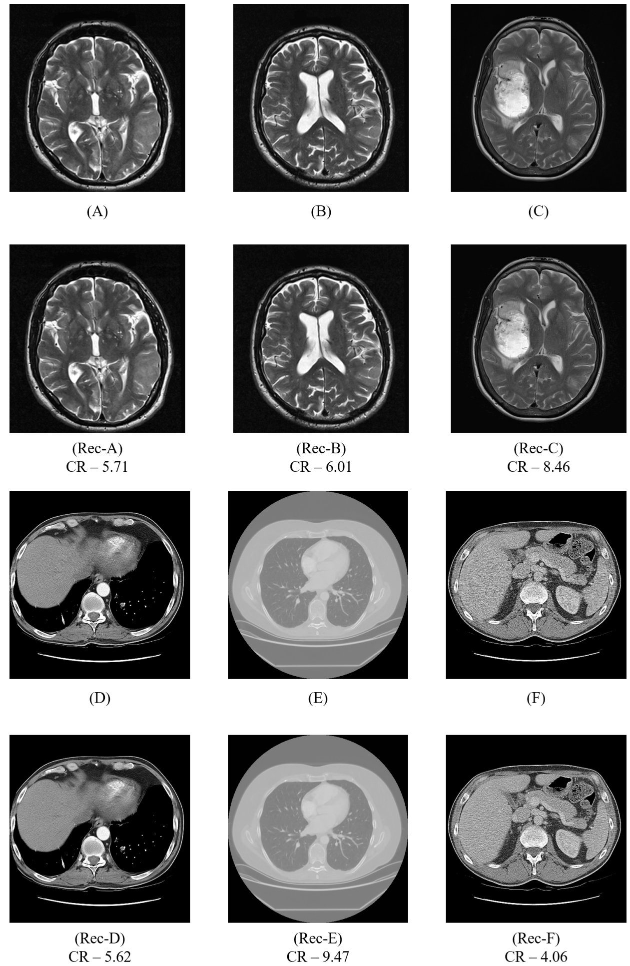

Fig. 16: Sample images from the DICOM image set and their Reconstructions from MDWT-L compression for target MSE ≈ 225. The reconstruction of A is denoted as Rec-A etc. (All images presented here are converted to jpg.)

and matrix traversal. The complexity of these custom components is proportional to the total number of elements in the matrix which is comparable to the overall pixel count in the image. Also, it contains loops that run for a constant number of iterations and other components that invoke some MATLAB built-in functions which cannot be directly assessed due to the absence of specific implementation or complexity documentation. Thus, a precise evaluation of the overall complexity is challenging without comprehensive information on such built-in functions.

The current implementation is designed specifically for 16-bit greyscale DICOM images. As future work, this could be extended for RGB DICOM images. Additionally, further studies can be carried out to evaluate comparisons with other algorithms and investigate the applicability of different quantization techniques.

V. Conclusion

Through this research, multiple modifications were implemented and investigated for Discrete Wavelet transform-based image compression in the DICOM Medical image domain. During implementation, first, the DICOM file was read and image data was separated from metadata. As the next step, image data was transformed into to frequency domain using discrete wavelet transform for analyzing and thresholding followed by quantization with the experimental modifications. Subsequently, entropy encoding was performed using run-length encoding along with DEFLATE-based gzip algorithm for the proposed modified variants whereas Huffman encoding was used for the general version. These modifications can be summarized as follows,

- Adaptive uniform scalar quantization
- RLE with DEFLATE for entropy encoding
- Multiple traversal mechanisms for RLE (Linear, Spiral and Diagonal)
- Use of RLE only based on the entropy of the coefficient matrices to minimize undesirable results

The experiments indicate noteworthy improvements in compression ratio while maintaining an equivalent level of quality by the modified variants compared to the general version; Discrete Wavelet Transform with Huffman encoding-based image compression. In the modified variants, the traversal mechanisms exhibit slight variations with mixed results when compared with each other.

Appendix A
Source Code and Data set

The source code and image data set can be found in the following GitHub repository.

https://github.com/Thisura24/DICOM-Image-Compress-MDWT

References

[1] "About DICOM: Overview," Dicomstandard.org. https://www.dicomstandard.org/about-home, (accessed May 11, 2024).

[2] S. W. Jahn, M. Plass, and F. Moinfar, "Digital pathology: advantages, limitations and emerging perspectives," *Journal of clinical medicine*, vol. 9, no. 11, p. 3697, 2020.

[3] G. Vijayvargiya, S. Silakari, and R. Pandey, "A survey: various techniques of image compression," *arXiv preprint arXiv:1311.6877*, 2013.

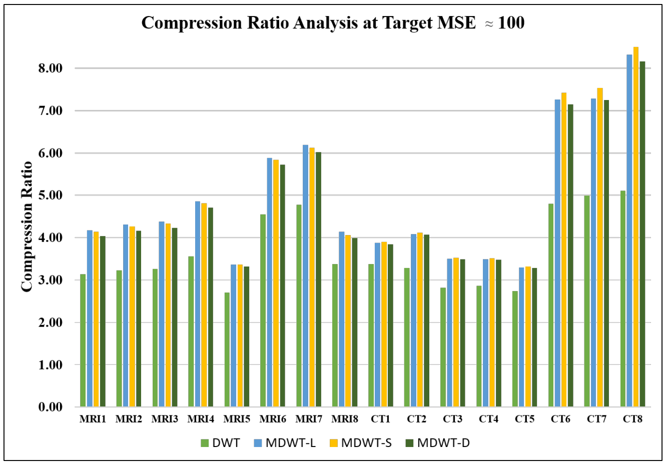

Fig. 17: Compression Ratio Analysis at Target MSE ≈ 100

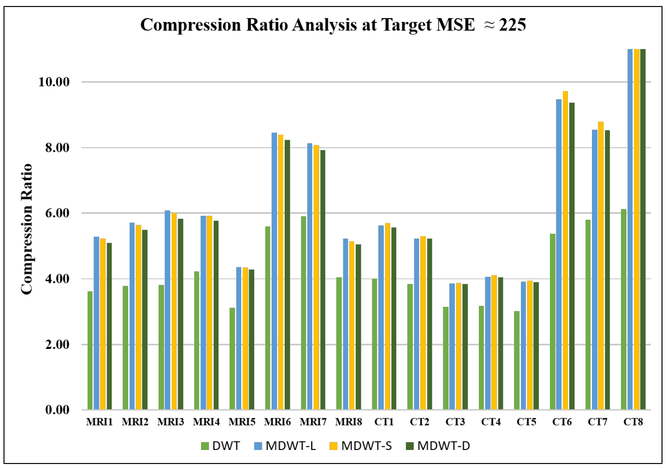

Fig. 18: Compression Ratio Analysis at Target MSE ≈ 225

[4] D. S. Taubman and M. W. Marcellin, "Jpeg2000: Standard for interactive imaging," *Proceedings of the IEEE*, vol. 90, no. 8, pp. 1336–1357, 2002.

[5] M. Mozammel, H. Chowdhury, and A. Khatun, "Image compression using discrete wavelet transform," *International Journal of Computer Science Issues*, vol. 9, 07 2012.

[6] A. Katharotiya, S. Patel, and M. Goyani, "Comparative analysis between dct & dwt techniques of image compression," *Journal of information engineering and applications*, vol. 1, no. 2, pp. 9–17, 2011.

[7] K. Bindu, A. Ganpati, and A. K. Sharma, "A comparative study of image compression algorithms," *International Journal of Research in Computer Science*, vol. 2, no. 5, p. 37, 2012.

[8] M. S. Ruchika, A. R. Singh, and A. Singh, "Compression of medical images using wavelet transforms," *International Journal of Soft Computing and Engineering*, vol. 2, no. 2, pp. 339–343, 2012.

[9] P. N. T. Ammah and E. Owusu, "Robust medical image compression based on wavelet transform and vector quantization," *Informatics in medicine unlocked*, vol. 15, p. 100183, 2019.

[10] H. Lee, "Wavelet analysis for image processing," *Institute of Communication Engineering, National Taiwan University, Taipei, Taiwan, ROC. On http://disp. ee. ntu. edu. tw/henry/wavelet_analysis. pdf*, 2017.

[11] "Read DICOM image - MATLAB wavedec2 - MathWorks India," in.mathworks.com. https://in.mathworks.com/help/wavelet/ref/wavedec2.html, (accessed May 11, 2024).

[12] Y. Zhang, W. Ding, Z. Pan, and J. Qin, "Improved wavelet threshold for image de-noising," *Frontiers in neuroscience*, vol. 13, p. 39, 2019.

[13] R. M. Gray and D. L. Neuhoff, "Quantization," *IEEE transactions on information theory*, vol. 44, no. 6, pp. 2325–2383, 1998.

[14] S. T. Kodukulla, "Lossless image compression using matlab: Comparative study," 2020.

[15] S. Oswal, A. Singh, and K. Kumari, "Deflate compression algorithm," *International Journal of Engineering Research and General Science*, vol. 4, no. 1, pp. 430–436, 2016.

[16] "Welcome to The Cancer Imaging Archive - The Cancer Imaging Archive (TCIA)," cancerimagingarchive.net. https://www.cancerimagingarchive.net/, (accessed May 12, 2024).